



PAPER • OPEN ACCESS

Effects of etching duration on silicon quantum dot size and photoluminescence quantum yield

To cite this article: Yizhou He *et al* 2024 *J. Phys.: Conf. Ser.* **2873** 012051

View the [article online](#) for updates and enhancements.

You may also like

- [Study on the influence factors of the grain growth type of micro-nano silver powders prepared by liquid-phase reduction method](#)
Xiaoling Ma, Jianwei Wang, Huijun He et al.
- [Innovative design of hole-carrying materials utilizing spiro-OMeTAD for halide hybrid perovskite solar cells](#)
Li Yang, Liqian Zhao, Liyun Cai et al.
- [Preparation of nano-TiO₂ spherical catalyst doped with nonmetallic elements for potential use in CO₂ reduction](#)
Yuan Yuan, Sirui Ruan, Yimng Ye et al.

ECS The Electrochemical Society
Advancing solid state & electrochemical science & technology

247th ECS Meeting
Montréal, Canada
May 18-22, 2025
Palais des Congrès de Montréal

Showcase your science!

Abstracts due December 6th

Effects of etching duration on silicon quantum dot size and photoluminescence quantum yield

Yizhou He¹, Qianxi Hao¹, Chi Zhang¹, Qi Wang¹, Wenxin Zeng¹, Jiamin Yu²,
Xue Yang^{2,*}, Xiaowei Guo^{1,3,*}, Shaorong Li¹, and Sergei K. Lazarouk⁴

¹School of Optoelectronic Science and Engineering, University of Electronic Science and Technology of China, Chengdu 610054, China

²China National Tobacco Corporation Sichuan Company, Chengdu, 610041, China

³Yangtze Delta Region Institute (Huzhou), University of Electronic Science and Technology of China, Huzhou 313001, China

⁴Belarusian State University of Informatics and Radioelectronics, P. Browka 6, Minsk 220013, Belarus

*Corresponding authors' e-mail: 280055419@qq.com (Xue Yang); gxw@uestc.edu.cn (Xiaowei Guo)

Abstract. The synthesis of silicon quantum dots (SiQDs) via thermal pyrolysis is considered promising due to its cost-effectiveness. The etching process in this method has the potential to control the size of SiQDs precisely and has thus garnered attention. However, there are varying observations regarding the effect of etching duration on SiQD size. Additionally, the impact of dioxonium hexafluorosilicate (DH), a byproduct of the etching process, on the photoluminescence (PL) quantum yield (QY) of SiQDs remains unclear. This study investigates the effect of etching duration on the physical and optical sizes as well as the PLQY of SiQDs. The results indicate that extending the etching duration decreases the physical size of SiQDs, while the optical size initially increases slightly before decreasing. The SiQDs transition through three phases with increasing etching duration: oxidation removal, shallow over-etching, and deep over-etching. Both amorphous silicon (a-Si) in the oxidation removal phase and DH in the deep over-etching phase act as non-radiative recombination centers, thereby reducing the PLQY of SiQDs. Therefore, optimizing the etching duration to achieve the shallow over-etching phase is essential. This study provides new insights into the effects of etching duration on SiQD size and PLQY, aiding in the preparation of higher-quality SiQDs.

1. Introduction

Silicon is the second most abundant element in the Earth's crust, next to oxygen, and has been utilized in various fields such as microelectronics [1], photovoltaics [2], and photodetection [3]. Despite its extensive usage in some areas, its indirect bandgap nature causes an extremely low photoluminescence (PL) quantum yield (QY) of bulk silicon, rendering it unsuitable for applications such as display and lighting [4]. However, the emergence of silicon quantum dots (SiQDs) solves this predicament as they possess more than two orders of magnitude higher PLQY than bulk silicon [4]. The high PLQY of SiQDs results from the quantum confinement effect, which gives silicon a quasi-direct transition property when the dimension of bulk silicon is reduced to a Bohr radius comparable to that of its excitons [5]. Researchers have developed a variety of strategies to synthesize SiQDs, including electrochemical



Si wafer etching [6], laser ablation of solid silicon [7], reduction reaction of halosilanes [8], plasma synthesis [9], and thermal pyrolysis [10, 11]. Among these methods, thermal pyrolysis stands out as the most promising pathway for SiQD synthesis due to its cost-effectiveness and ability to produce high-quality SiQDs [10-12].

The etching process is a crucial stage that has garnered attention as alterations in its conditions are anticipated to influence the size of SiQDs [12-15]. Henderson et al. observed a notable blue shift (~200 nm) in the PL spectra of SiQDs with prolonged hydrofluoric acid (HF) etching duration (35~65 min), indicating a reduction in the SiQD size [13]. In contrast, Rodríguez Nunez et al. presented differing results regarding the etching process [14]. They discovered that as the etching duration increased (1~10 h), the PL spectra of SiQDs exhibited a blue shift (≤ 160 nm) only in the presence of illumination, remaining unaltered in darkness. This phenomenon is ascribed to an accelerated etching rate stemming from exciton production under conditions of low oxidation rate. Subsequently, Chandra et al. identified the formation of the byproduct dioxonium hexafluorosilicate (DH) with prolonged etching duration [15]. However, the formation mechanism of DH and its impact on the photoluminescence properties of SiQDs is still lacking. Recently, Zhou et al. observed a consistent blue shift (60~120 nm) in the PL spectra of SiQDs with increasing etching duration (1~6 h) [12]. They also found that extending the etching duration resulted in a ~25% decrease in the PLQY of the SiQDs. However, the mechanism underlying the effect of extended etching duration on the PLQY remains unclear. Additionally, there are different claims regarding whether extending the etching duration reduces the diameter of SiQDs.

In this study, we investigated the effect of HF etching duration on the physical and optical diameters of SiQDs derived from pyrolysis products, as well as on their PLQYs.

2. Experiments

The synthesis of SiQDs is sequentially divided into four steps: hydrolysis-condensation, thermal pyrolysis, HF etching, and hydrosilylation [11]. In the hydrolysis-condensation stage, HSQ polymers were obtained by mixing triethoxysilane (TES) with water at pH=3. During the pyrolysis stage, the HSQ polymer was introduced into a tube furnace and maintained at 1000°C for 2 hours under a carrier gas mixture of 5% hydrogen (H₂) and 95% argon (Ar) to obtain the pyrolysis product. For the HF etching stage, the pyrolysis product was placed in a polytetrafluoroethylene (PTFE) bottle. To this, 16 ml of 48% hydrofluoric acid and 10 ml of ethanol were added. The bottle was sealed, and the mixture was subjected to magnetic stirring in the dark for 30, 45, and 120 minutes to obtain hydride SiQDs (H-SiQDs). During the hydrosilylation stage, the hydrosilylation reaction was performed using 1-octadecene on the three samples to yield the corresponding octadecyl-passivated SiQDs (OD-SiQDs).

3. Results and discussions

Figure 1(a) displays X-ray diffraction (XRD) spectra of the pyrolysis products both before and after etching. The diffraction peaks at 22°, 28°, 47°, and 56° observed in the pyrolysis products correspond to the (111) crystal plane of SiO₂ and the (111), (220), and (311) crystal planes of Si with a diamond structure [12, 15], indicating the presence of SiQDs embedded in the SiO₂ matrix as reported in previous studies [12, 15]. The diffraction peaks of SiO₂ completely disappear after 30, 45, and 120 min of etching, confirming the successful removal of the SiO₂ matrix after 30 min of etching. However, in addition to the diffraction peaks of liberated Si, a peak at 18° is observed, corresponding to DH, which has also been reported in the study of Chandra et al [15]. The intensity of this peak increases with increasing etching duration while the intensity of the peak of silicon decreases, suggesting that DH is formed as a result of the etching effect of HF on SiQDs. Additionally, the presence of more yellow impurities is observed with increasing etching duration, particularly after 120 min of etching, which is consistent with an increase in the proportion of DH indicated by the diffraction peaks. The reaction of HF to DH is shown below:



Figure 1(b) presents the full width at half maximum (FWHM) values of the silicon diffraction peaks of the pyrolysis product after etching. The Scherrer equation is then applied to calculate the average crystal size (d_{XRD}) of the SiQDs as illustrated in Figure 1(c) [16]. The d_{XRD} of the pyrolysis products are 4.51 nm, 4.13 nm, and 3.29 nm after etching for 30, 45, and 120 min, respectively. This further corroborates the HF etching of SiQDs. The Raman spectrum of the pyrolysis product, shown in Figure 1(d), consists of crystalline silicon (c-Si, 499 cm^{-1}) and amorphous silicon (a-Si, 480 cm^{-1}) [17, 18], with a crystalline fraction of 94.68%. Additionally, the Raman peak of the c-Si part is shifted $\sim 20\text{ cm}^{-1}$ compared to the c-Si wafers, arising from the difference in Raman spectra between SiQDs and bulk silicon [17, 18].

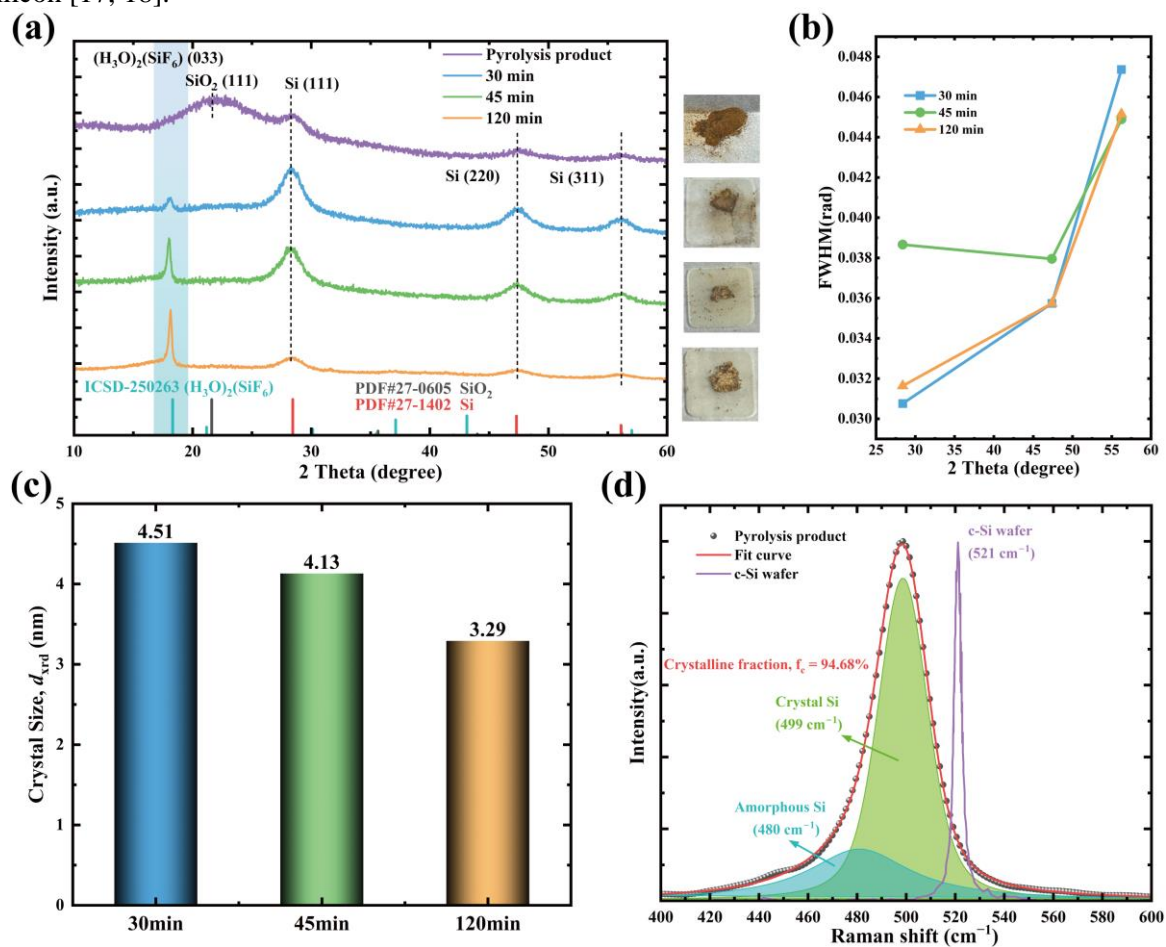


Figure 1. (a) XRD patterns of pyrolysis products before and after etching for 30, 45, 120 min (insets are the corresponding photographs); (b) FWHM values of the silicon diffraction peaks of the pyrolysis product after etching for 30, 45, 120 min; (c) Average crystal size (d_{XRD}) of the SiQDs etched for 30, 45, 120 min; (d) Raman spectra of the pyrolysis product (crystalline and amorphous fractions were fitted by Voigt function).

OD-SiQDs were synthesized using octadecene as a ligand for the hydrosilylation of H-SiQDs. Figures 2(a) and (b) present transmission electron microscopy (TEM) images of OD-SiQDs etched for 30 and 45 min. The frequency distribution of SiQD sizes indicates average particle sizes (d_{TEM}) of $5.52 \pm 0.08\text{ nm}$ and $4.77 \pm 0.18\text{ nm}$, as shown in Figures 2(e) and (f). Additionally, Figures 2(c) and (d) show high-resolution TEM (HRTEM) images of OD-SiQDs etched for 30 and 45 min, with white circles highlighting the OD-SiQDs. The observed lattice spacing of 0.31 nm corresponds to the d-spacing of the Si (111) crystal plane [19].

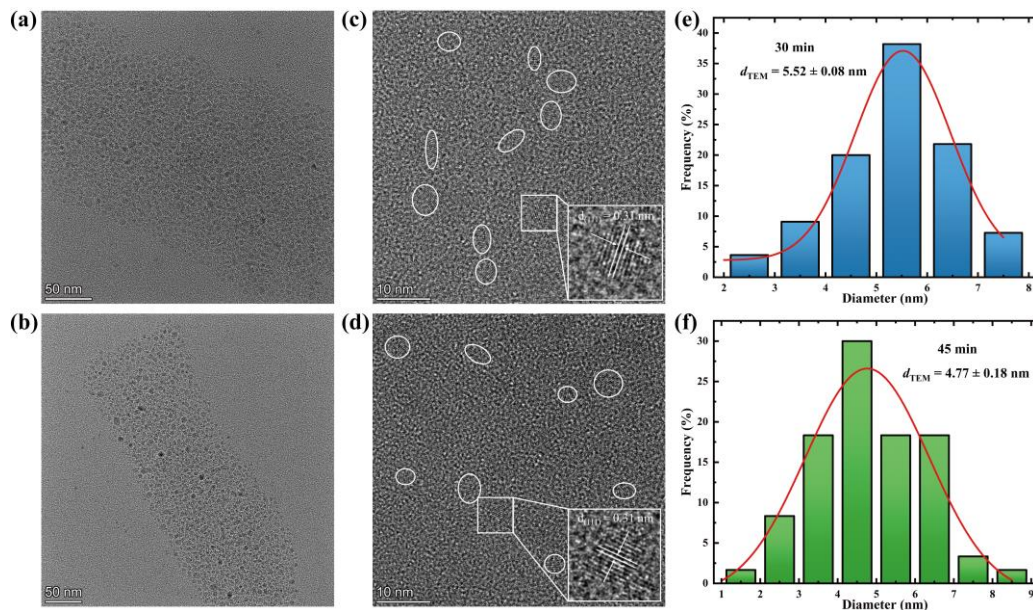


Figure 2. (a-b) TEM images of OD-SiQDs etched for 30 min and 45 min; (c-d) HRTEM images of OD-SiQDs etched for 30 min and 45 min; (e-f) Frequency distribution of OD-SiQD sizes.

Figure 3(a) presents the PL spectra of OD-SiQDs for various etching durations, with the inset showing a photograph of OD-SiQDs etched for 45 min. Figure 3(b) illustrates the shifts in PL peaks, demonstrating that the PL peaks of OD-SiQDs etched for 30, 45, and 120 min are centered at 900 nm, 911 nm, and 872 nm, respectively. Using the effective mass approximation (EMA) method [5], the optical diameters (d_{OPT}) of these OD-SiQDs were calculated to be 5.16 nm, 5.42 nm, and 4.42 nm, respectively. Figure 3(c) summarizes the d_{XRD} , d_{TEM} , and d_{OPT} for etching durations of 30, 45, and 120 min. Both the Scherrer equation and the EMA method provide approximate means of estimating crystal diameters [11, 16], resulting in deviations from the true values. Therefore, it is more valuable to focus on the trends rather than on specific values. The trends in d_{XRD} and d_{TEM} indicate that increasing the etching duration reduces the physical size of the SiQDs. This phenomenon, differing from the results of Rodríguez Nunez et al. [14], who conducted etching in the dark but consistent with several other studies [12, 13], is attributed to the high oxidation rate of the etching solution used [14]. However, d_{OPT} shows an opposite trend for the 30 and 45-min etching durations. Veinot and colleagues demonstrated that the a-Si in SiQDs forms a shell on the c-Si surface [16, 20]. Therefore, HF preferentially removes the a-Si shells from the c-Si during etching. Since d_{XRD} decreases from 30 to 45 min, this suggests the a-Si shell is no longer present at 45 min; otherwise, d_{XRD} at 45 min would remain unchanged compared to that at 30 min if the shell were still present. The XRD pattern of SiQDs etched for 30 min shows a small amount of DH, indicating the HF etching reaction is at an early stage. It is reasonable to speculate that an a-Si shell remains on the SiQDs etched for 30 min, resulting in a large number of defects at the c-Si/a-Si interface that tend to trap electrons and holes for nonradiative recombination [16]. Furthermore, electrons and holes generated near the interface (on the c-Si side) are also easily trapped, reducing the effective diameter for radiative recombination compared to the actual c-Si diameter. This explains the discrepancy between the trends of d_{XRD} and d_{OPT} for short etching durations (30~45 min). Figure 3(d) presents the PL decay profiles of OD-SiQDs. The average lifetimes of PL decay at the microsecond level (82.93 μ s, 88.46 μ s, and 67.91 μ s) were obtained through bi-exponential fitting, indicating that these PL emissions originate from intrinsic radiation induced by the SiQD cores rather than by surface groups [4, 5]. Figure 3(e) illustrates the PLQYs of 6.43%, 18.87%, and 10.89% for OD-SiQDs etched for 30, 45, and 120 minutes, respectively. The radiative recombination coefficient (k_r) and non-radiative recombination coefficient (k_{nr}) can be calculated using the following equation [17]:

$$\text{PLQY} = \frac{k_r}{k_r + k_{nr}} = k_r \tau \quad (2)$$

As shown in Figure 3(f) and Table 1, the 45-min OD-SiQDs exhibit the highest k_r of 2133 s^{-1} and the lowest k_{nr} of 9171 s^{-1} , corresponding to the highest PLQY. The 30-min OD-SiQDs have a smaller k_r and larger k_{nr} compared to the 45-min OD-SiQDs due to the defects of both a-Si and c-Si/a-Si interface acting as nonradiative recombination centers, enhancing nonradiative recombination and weakening radiative recombination. This observation further supports the existence of a-Si shells. The smaller k_r and larger k_{nr} in the 120-min OD-SiQDs are due to the significant amount of DH generated by over-etching, which is adsorbed on the SiQDs and serves as nonradiative recombination centers, capturing the electrons and holes generated in the SiQDs. Additionally, the DH adsorbed on the SiQDs may absorb UV light intended for the SiQDs or the PL emitted from the SiQDs, causing the excited excitons to undergo nonradiative recombination within the DH. For the 45-min OD-SiQDs, although a middle amount of DH is present as recombination centers, a significant number of a-Si-related recombination centers are removed, leading to an increase in PLQY.

Based on the above discussion, a possible reaction mechanism for the etching process is illustrated in Figure 4. After 30 min of etching, the SiO_2 matrix is completely removed from the pyrolysis product, a stage termed the oxidation removal state. After 45 min of etching, the a-Si shell is removed, and the c-Si core is etched and reduced in size, referred to as the shallow over-etching state. After 120 min of etching, the c-Si core is further etched, reducing its size even more, a stage termed the deep over-etching state. The d_{XRD} and d_{TEM} of SiQDs consistently decrease as the etching reaction progresses, whereas d_{OPT} initially increases slightly and then decreases. Both the oxidation removal state and the deep over-etching state result in significant amount of nonradiative recombination centers (a-Si and DH), reducing the PLQY. In contrast, the shallow over-etching state contains only a middle amount of DH as nonradiative recombination centers, thereby increasing the PLQY compared to the other states.

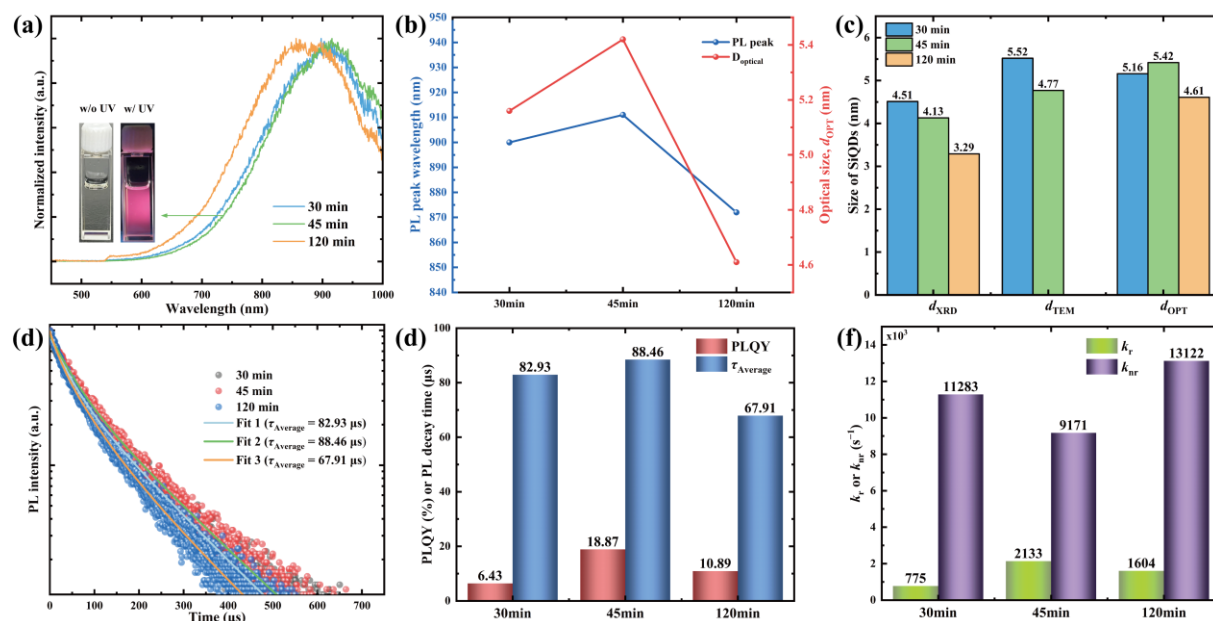
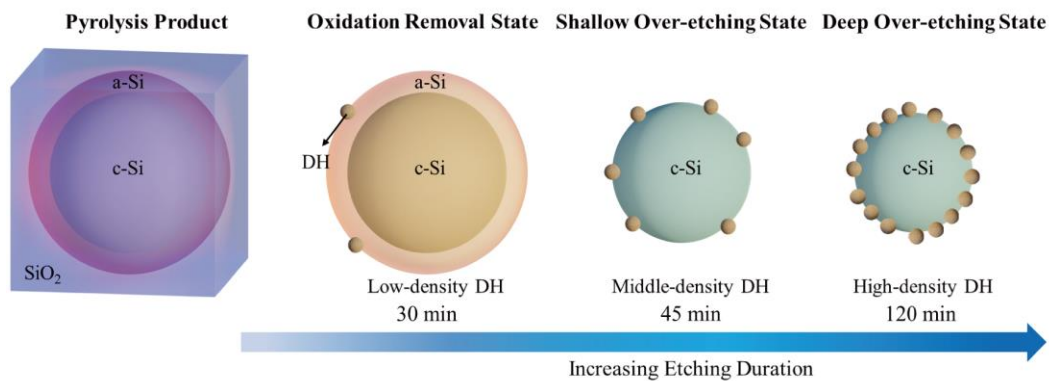


Figure 3. (a) PL spectra of SiQDs obtained at different etching durations; (b) PL peak wavelength and corresponding optical dimensions of SiQDs obtained at different etching durations; (c) Average crystal size (d_{XRD}), average particle size (d_{TEM}), and optical diameter (d_{OPT}) of the prepared SiQDs; (d) PL decay profiles of SiQDs obtained at different etching durations; (e) PLQYs and PL decay average lifetimes of the SiQDs; (f) k_r and k_{nr} of the SiQDs.

Table 1. Characteristic parameters of SiQDs obtained at different etching durations.

Etching duration (min)	d_{XRD} (nm)	d_{TEM} (nm)	d_{OPT} (nm)	τ (μs)	PLQY (%)	k_r (s^{-1})	k_{nr} (s^{-1})
45	4.51	5.52	5.16	82.93	6.43	775	11283
90	4.13	4.77	5.42	88.46	18.87	2133	9171
120	3.29	/	4.61	67.91	10.89	1604	13122

**Figure 4.** (a) Schematic diagram of the reaction mechanism for pyrolysis products with increasing etching duration.

4. Conclusion

We investigated the effect of HF etching duration on SiQDs using XRD spectroscopy, Raman spectroscopy, TEM analysis, and PL spectroscopy. Our findings indicate that the physical size of the SiQDs decreases continuously with extended HF etching time, while the optical size initially increases slightly and then decreases. This phenomenon is attributed to the trapping of electrons and holes generated near the c-Si/a-Si interface, reducing the effective radiative recombination diameter. The SiQDs released by etching would be in three phases sequentially with increasing etching duration: oxidation removal state, shallow over-etching state, and deep over-etching state. Notably, the a-Si in the oxidation removal state and the large amount of DH in the deep over-etching state act as non-radiative recombination centers, thus reducing the PLQY of SiQDs. Therefore, selecting an appropriate etching duration to achieve the shallow over-etching state is crucial for improving the PLQY of SiQDs.

Acknowledgements

This project was supported by China National Tobacco Corporation Sichuan Branch (SCYC202120) and Sichuan Science and Technology Program (2022ZYD0110).

References

- [1] Venema L 2011 *Nature* **479** 309 [CrossRef].
- [2] Lin H, Yang M, Ru X, Wang G, Yin S, Peng F, Hong C, Qu M, Lu J, Fang L, Han C, Procel P, Isabella O, Gao P, Li Z and Xu X 2023 *Nat. Energy* **8** 789-99 [CrossRef].
- [3] Berencén Y, Prucnal S, Liu F, Skorupa I, Hübner R, Rebohle L, Zhou S, Schneider H, Helm M and Skorupa W 2017 *Sci. Rep.* **7** 43688 [CrossRef].
- [4] Saitow K-i 2024 *B. Chem. Soc. Jpn.* **97** uoad002 [CrossRef].
- [5] Ni Z, Zhou S, Zhao S, Peng W, Yang D and Pi X 2019 *Mat. Sci. Eng. R.* **138** 85-117 [CorssRef].
- [6] Lazarouk S, Jaguiro P, Katsouba S, Maiello G, La Monica S, Masini G, Proverbio E and Ferrari A 1997 *Thin Solid Films* **297** 97-101 [CrossRef].

- [7] Kabashin A V, Singh A, Swihart M T, Zavestovskaya I N and Prasad P N 2019 *ACS Nano* **13** 9841-67 [CrossRef].
- [8] Li Q, Luo T-Y, Zhou M, Abroshan H, Huang J, Kim H J, Rosi N L, Shao Z and Jin R 2016 *ACS Nano* **10** 8385-93 [CrossRef].
- [9] Kortshagen U R, Sankaran R M, Pereira R N, Girshick S L, Wu J J and Aydil E S 2016 *Chem. Rev.* **116** 11061-127 [CrossRef].
- [10] Cheong I T, Mock J, Kallergi M, Groß E, Meldrum A, Rieger B, Becherer M and Veinot J G C 2023 *Adv. Opt. Mater.* **11** 2201834 [CrossRef].
- [11] Ueda H and Saitow K-i 2024 *ACS Appl. Mater. Interfaces* **16** 985-97 [CrossRef].
- [12] Zhou J, Huang J, Chen H, Samanta A, Linnros J, Yang Z and Sychugov I 2021 *J. Phys. Chem. Lett.* **12** 8909-16 [CrossRef].
- [13] Henderson E J, Kelly J A and Veinot J G C 2009 *Chem. Mater.* **21** 5426-34 [CrossRef].
- [14] Rodríguez Núñez J R, Kelly J A, Henderson E J and Veinot J G C 2012 *Chem. Mater.* **24** 346-52 [CrossRef].
- [15] Chandra S, Ghosh B, Beaune G, Nagarajan U, Yasui T, Nakamura J, Tsuruoka T, Baba Y, Shirahata N and Winnik F M 2016 *Nanoscale* **8** 9009-19 [CrossRef].
- [16] Cheong I T, Yang Szepesvari L, Ni C, Butler C, O'Connor K M, Hooper R, Meldrum A and Veinot J G C 2024 *Nanoscale* **16** 592-603 [CrossRef].
- [17] Ono T, Xu Y, Sakata T and Saitow K-i 2022 *ACS Appl. Mater. Interfaces* **14** 1373-88 [CrossRef].
- [18] Terada S, Xin Y and Saitow K-i 2020 *Chem. Mater.* **32** 8382-92 [CrossRef].
- [19] Lu S, Wu B, Sun Y, Cheng Y, Liao F and Shao M 2017 *J. Mater. Chem. C* **5** 6713-7 [CrossRef].
- [20] Thiessen A N, Zhang L, Oliynyk A O, Yu H, O'Connor K M, Meldrum A and Veinot J G C 2020 *Chem. Mater.* **32** 6838-46 [CrossRef].